

SUSY interpretation of the Egret GeV anomaly, Xenon-10 dark matter search limits and the LHC

Howard Baer^{1*}, Alexander Belyaev^{2†} and Heaya Summy^{1*}

1. *Dept. of Physics, Florida State University, Tallahassee, FL 32306, USA*
2. *School of Physics and Astronomy, University of Southampton, Southampton, SO17 1BJ, UK*

Abstract

The observation of the Egret experiment of an excess of diffuse gamma rays with energies above $E_\gamma = 1$ GeV has previously been interpreted in the context of the minimal supergravity model (mSUGRA) as coming from neutralino annihilation into mainly b -quarks in the galactic halo, with neutralino mass in the vicinity of 50-70 GeV. We observe that in order to obtain the correct relic abundance of neutralinos in accord with WMAP measurements, the corresponding neutralino-proton direct detection (DD) rates should be in excess of recent limits from the Xenon-10 collaboration. While it does not appear possible to satisfy the Egret, WMAP and Xenon-10 constraints simultaneously within the mSUGRA model, we find that it is easily possible in models with non-universal Higgs soft masses (NUHM). In either case, gluino pair production from $m_{\tilde{g}} \sim 400 - 500$ GeV should occur at large rates at the CERN LHC, and a gluino pair production signal should be visible with just 0.1 fb^{-1} of integrated luminosity. The NUHM interpretation predicts a rather light spectrum of heavy Higgs bosons with $m_A \sim 140 - 200$ GeV over the whole parameter space which would interpret Egret data. Spin-independent DD rates are predicted to be just above 10^{-8} pb, within range of the next round of direct dark matter detection experiments.

PACS numbers: 14.80.Ly, 12.60.Jv, 11.30.Pb

*Email: baer@hep.fsu.edu

†Email: a.belyaev@phys.soton.ac.uk

*Email: heaya@hep.fsu.edu

1 Introduction

An abundance of astrophysical evidence points to the conclusion that the bulk of the matter in the universe is composed *not* of Standard Model (SM) particles, but of some unknown non-relativistic elementary particle known as cold dark matter (CDM)[1]. An analysis of the three-year WMAP and galaxy survey data sets[2] implies that the ratio of cold dark matter density to critical density,

$$\Omega_{CDM}h^2 \equiv \rho_{CDM}/\rho_c = 0.111_{-0.015}^{+0.011} \quad (2\sigma). \quad (1)$$

where $h = 0.74 \pm 0.03$ is the scaled Hubble constant. While the density of CDM is becoming precisely known, the identity of the CDM particle (or particles) is still a complete mystery. Although numerous candidate CDM particles populate the theoretical literature, the WIMPs (weakly interacting massive particles) stand out in that their thermal abundance can be calculated, and is found to be in rough accord with Eq. (1) provided the WIMP mass is of order 100-1000 GeV. Of the numerous WIMP candidates in the literature, the lightest neutralino of supersymmetric (SUSY) theories is especially popular because SUSY solves a host of theoretical problems associated with the SM, and also receives some (albeit indirect) support from data (in the form of the measured gauge couplings unifying at $Q = M_{GUT}$ under MSSM RG evolution and also from other precision electroweak measurements[3]).

There is at present a multi-pronged effort aimed at identifying WIMP dark matter particles and measuring their properties[4]. The most direct approach is to try to detect relic WIMPs left over from the Big Bang by observing WIMP-nucleon collisions in experiments located deep underground. Limits from the CDMS[5] experiment and more recently from the Xenon-10[6] experiment have begun probing the upper limits of SUSY model parameter space.

WIMP particles can also be searched for at collider experiments such as those at the CERN LHC, especially if the dark matter particle is but one of a whole family of particles, some of which can be produced via strong and electromagnetic interactions. The dark matter particle would then be produced by cascade decays of heavier particles, and would lead to missing transverse energy in collider events. Such is the case of theories such as R -parity conserving supersymmetry[7], KK -parity conserving universal extra dimensions (UED)[8] and little Higgs models with T -parity[9].

Dark matter may also be searched for indirectly. For instance, the sun can sweep up WIMP particles as it traverses its galactic orbit, so that WIMPs accumulate at a high density in the solar core. Then WIMP-WIMP annihilation to SM particles can occur at high rates in the solar core. While most SM particles would be absorbed by the surrounding solar medium, multi-GeV scale ν_μ s would escape and later convert to muons in neutrino telescopes such as Amanda/IceCube or Antares.

In addition, dark matter in the galactic halo can be searched for indirectly via its annihilation into high energy gamma rays or anti-matter. In the case of gamma rays, searches look either for WIMP-WIMP annihilation directly to $\gamma\gamma$ pairs (loop-suppressed since WIMPs are electrically neutral) or via WIMP-WIMP annihilation to $q\bar{q}$ pairs, followed by $q \rightarrow \pi^0 \rightarrow \gamma\gamma$ via hadronization and decay. In the latter case, one expects a diffuse spectrum of gamma rays with energies $E_\gamma < M_{WIMP}$ atop a background arising from cosmic ray spallation onto nuclei, inverse Compton scattering and bremsstrahlung.

The spectral shape of the gamma ray sky has been measured in the 1990s by the Egret experiment in the energy range of 0.1-10 GeV[10], where already an excess of signal with $E_\gamma > 1$ GeV above expected background was noted. The $E_\gamma > 1$ GeV excess apparently is seen in all sky directions. An analysis by de Boer *et al.*[11] explains the Egret GeV anomaly as coming from neutralino annihilation in the galactic halo into mainly $b\bar{b}$ pairs. A fit of the neutralino hypothesis to the Egret data favor a neutralino in the mass range $m_{\tilde{Z}_1} \sim 50 - 70$ GeV. On the astrophysics side of the de Boer *et al.* interpretation, the strength of the signal depends on the dark matter density distribution throughout the galaxy. In order to explain the Egret GeV anomaly, de Boer *et al.* invoke a DM density distribution involving two rings of dark matter at 4 and 13 kpc[12].

De Boer *et al.* further interpret the apparent WIMP annihilation signal in the context of the minimal supergravity (mSUGRA) model[13], which allows a complete determination of all super-particle and Higgs boson masses and mixings in terms of just a few parameters[14]

$$m_0, m_{1/2}, A_0, \tan\beta \text{ and } \text{sign}(\mu), \quad (2)$$

where m_0 is a common scalar mass at energy scale $Q = M_{GUT}$, $m_{1/2}$ is the common gaugino mass at M_{GUT} , A_0 the common trilinear GUT-scale soft breaking mass, $\tan\beta$ is the ratio of higgs vevs and μ is the superpotential Higgs mass parameter. The magnitude— but not the sign— of the μ term is determined by constraints arising from requiring an appropriate breakdown of electroweak symmetry in the mSUGRA model. In mSUGRA, once the GUT scale soft SUSY breaking terms are stipulated at M_{GUT} , their weak scale values can be calculated via renormalization group equations (RGEs). The physical SUSY particle masses and mixings can then be calculated in terms of the weak scale soft SUSY breaking terms via well-known algorithms[7].

To generate a neutralino WIMP with mass 50-70 GeV, de Boer *et al.* require $m_{1/2}$ in the range of 130-170 GeV. This rather low value of $m_{1/2}$ typically leads to light Higgs masses $m_h \lesssim 114.4$ GeV (the limit from LEP2 on SM-like Higgs scalars) and to large contributions to the branching fraction $BF(b \rightarrow s\gamma)$. To avoid these constraints, de Boer *et al.* adopt a large value of $m_0 \sim 1500$ GeV[15]. Then, to gain accord with the measured relic density (Eq. 1), they require large $\tan\beta \sim 54$. For such a large value of $\tan\beta$, the b -quark and τ -lepton Yukawa couplings become very large, the pseudoscalar Higgs mass m_A falls, and its width grows. Neutralinos \tilde{Z}_1 can then annihilate efficiently in the early universe as $\tilde{Z}_1\tilde{Z}_1 \rightarrow b\bar{b}$ via *virtual, non-resonant* A exchange in the s -channel[16]. Just as neutralinos can annihilate efficiently via A^* in the early universe, so can they annihilate efficiently via A^* to $b\bar{b}$ in the galactic halo, since the A -annihilation diagrams are s -wave (while h, H annihilation is p -wave, and thus velocity-suppressed). The dominant halo annihilation $\tilde{Z}_1\tilde{Z}_1 \rightarrow A^* \rightarrow b\bar{b} \rightarrow \pi^0 \rightarrow \gamma$ can then describe the Egret gamma ray excess. Note that there is little uncertainty in the gamma spectrum from 50-70 GeV WIMP annihilation, since the corresponding process $e^+e^- \rightarrow b\bar{b} \rightarrow \gamma$ has been well-measured at LEP/LEP2.

It is important to note that several alternative explanations/insights regarding the Egret excess have emerged[17].

- In Ref. [18], Strong, Moskalenko and Reimer verify that a “conventional model” of cosmic ray production and propagation is insufficient to explain the Egret GeV anomaly, even

if augmented by hard sources of additional cosmic ray production in the inner galaxy. However, by suitably adjusting the spectrum of cosmic protons and electrons, they find they *are* able to by-and-large match the Egret data.

- Alternatively, Stecker *et al.*[19] claim the Egret excess can be explained by a calibration error in Egret gamma measurements with $E_\gamma > 1$ GeV. This would explain why an excess of high energy gammas comes from all sky regions.
- Bergstrom *et al.*[20] point out that if they use the deBoer derived distribution of galactic dark matter, including the ring structure, then the SUSY region favored in the deBoer analysis yields an anti-proton flux far in excess of measurements from the BESS experiment. These calculations adopt the isotropic DarkSUSY model of cosmic ray propagation. DeBoer *et al.* counter that using an *anisotropic* model of galactic cosmic ray propagation would greatly reduce the expected \bar{p} flux[21].

In this note, we wish to examine the SUSY interpretation of the Egret excess, and compare it with other constraints on sparticle masses. We find that the SUSY interpretation in terms of the mSUGRA model is in conflict with recent results on direct detection of dark matter from the Xenon-10 experiment. By moving to models with non-universality in the Higgs sector, however, one may preserve the SUSY interpretation of the Egret gamma ray excess, while staying below bounds on direct detection of DM. In any case, the imminent turn-on of the LHC should decide the issue. The deBoer interpretation predicts gluinos with mass $m_{\tilde{g}} \sim 400 - 500$ GeV. Production cross sections for gluino pair production in this mass range at the LHC are at the 10^5 fb level. Thus, LHC should decisively test the deBoer scenario with as little as 0.1 fb $^{-1}$ of integrated luminosity. If the mSUGRA interpretation is correct, then the heavy Higgs boson A should have mass around $200 - 400$ GeV. If an interpretation in terms of the NUHM model is correct, then m_A should be much lower- in the $140 - 200$ GeV range.

2 Confronting SUSY interpretation of Egret GeV anomaly with Xenon-10 direct dark matter search

2.1 mSUGRA analysis

We begin by calculating sparticle mass spectra using the Isajet 7.76[22] Isasugra code. Isajet begins with weak scale \overline{DR} values for the three gauge couplings and Yukawa couplings, and evolves up in energy to determine M_{GUT} , defined as the Q value where gauge couplings $g_1 = g_2$. At M_{GUT} , soft SUSY breaking boundary conditions are input, and the set of 26 coupled 2-loop RGEs are evolved down to M_{weak} . Beta-function threshold effects are included in the 1-loop portion of RGEs for gauge and Yukawa couplings, giving a smooth transition between MSSM and SM effective theories. All soft terms which mix are frozen out at scale $M_{SUSY} = \sqrt{m_{\tilde{t}_L} m_{\tilde{t}_R}}$, while all non-mixing soft terms are frozen out at their own mass scale (*e.g.* $m_{\tilde{u}_R}^2$ stops running when $Q = m_{\tilde{u}_R}$ is reached[23]). The RG-improved 1-loop MSSM scalar potential is minimized at $Q = M_{SUSY}$, which determines the value of μ^2 . All tree level sparticle masses are computed. Once these are known, then all 1-loop sparticle masses are computed, including

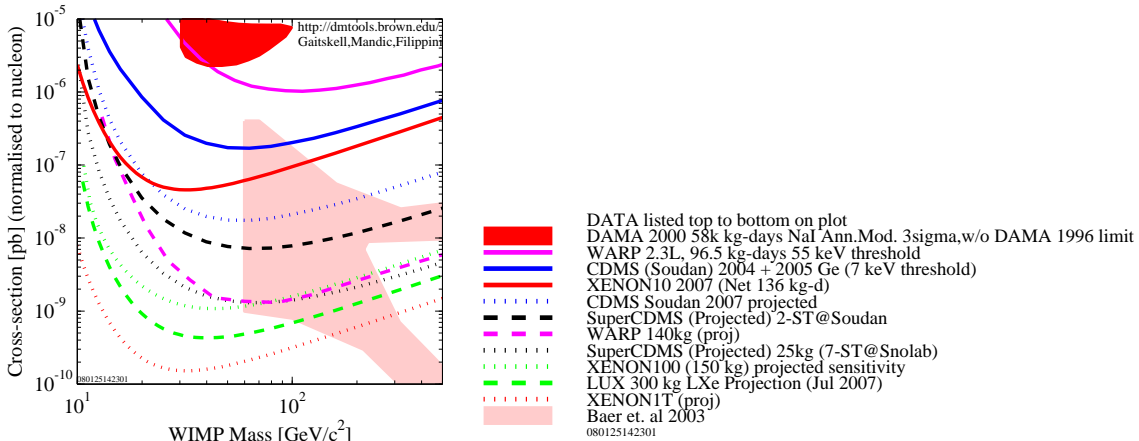


Figure 1: *Plot of reach of various present and future dark matter direct detection experiments compared to theory prediction in the mSUGRA model.*

SUSY threshold corrections to m_t , m_b and m_τ . The threshold effects alter the trajectories of the running couplings, so that an up-down iterative approach is used to calculate all 1-loop corrected sparticle masses; the iterations terminate when a convergence criterion is satisfied. At this point, all sparticle decay branching fractions are calculated, along with neutralino relic density $\Omega_{\tilde{Z}_1} h^2$, $a_\mu = (g - 2)_\mu/2$, $BF(b \rightarrow s\gamma)$, $\sigma_{SI}(\tilde{Z}_1 p)$, $BF(B_s \rightarrow \mu^+ \mu^-)$ and $\langle \sigma v \rangle|_{v \rightarrow 0}$, via the Isatools package[24]. The latter quantity, the neutralino annihilation cross section times relative velocity, in the limit as $v \rightarrow 0$, is the crucial particle physics quantity needed to evaluate various halo annihilation processes.

Regarding the neutralino direct dark matter detection cross section, we note here that a new limit on the spin-independent neutralino-nucleon scattering cross section, $\sigma_{SI}(\tilde{Z}_1 p)$, has appeared from the Xenon-10 collaboration[6]. This new limit, displayed as the solid red curve in Fig. 1[25], excludes $\sigma_{SI}(\tilde{Z}_1 p) \gtrsim 6 \times 10^{-8}$ pb for $m_{\tilde{Z}_1} \sim 60$ GeV. We also show in this figure the projected reach of several future direct detection experiments (dashed curves), along with theoretical predictions from a scan over mSUGRA model parameter space[26] (pink region). The reach contours assume a standard local DM density of $\rho_{DM} = 0.3$ GeV/cm³, and a standard DM velocity profile.

We first attempt to verify the de Boer *et al.* suggested mSUGRA interpretation using the Isajet code. The requirement that $m_{\tilde{Z}_1} \sim 60$ GeV means that– in models with gaugino mass unification and $\mu \gg M_2$ – the lightest neutralino should be dominantly bino-like. The trick is to get a low relic density in accord with WMAP, while maintaining a large value of $\langle \sigma v \rangle|_{v \rightarrow 0}$, so there is sufficient neutralino annihilation in the galactic halo. The LEP2 constraints that *i*). $m_{\tilde{W}_1} > 103.5$ GeV and *ii*). $m_\tau \gtrsim 95$ GeV means that co-annihilation cannot be used to reduce the relic density to WMAP allowed levels. De Boer *et al.* suggest taking $m_{1/2} \sim 160$ GeV to get $m_{\tilde{Z}_1} \sim 60$ GeV, and large m_0 to suppress SUSY contributions to $BF(b \rightarrow s\gamma)$ and to raise the value of m_h to LEP2-allowed values¹. These input parameters, along with

¹Here, we require $m_h \gtrsim 111$ GeV to account for a roughly 3 GeV slop in the theory calculation of m_h , while

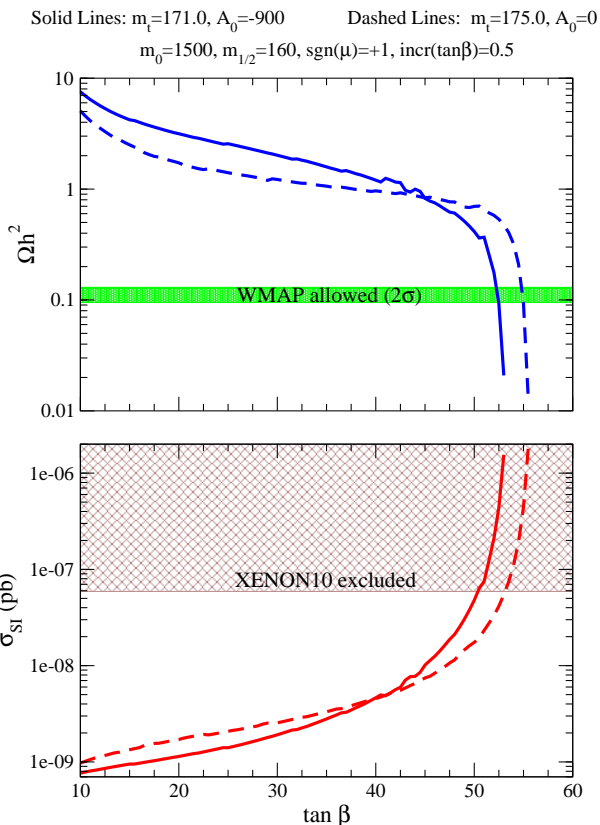


Figure 2: Plot of a). $\Omega_{\tilde{Z}_1} h^2$ versus $\tan\beta$ and b). $\sigma_{SI}(\tilde{Z}_1 p)$ versus $\tan\beta$ for two cases in the $mSUGRA$ model.

$A_0 = 0$ and $\tan\beta = 10$, give $\Omega_{\tilde{Z}_1} h^2 \sim 10$, which is two orders of magnitude higher than Eq. (1). In Fig. 2a., we plot the value of $\Omega_{\tilde{Z}_1} h^2$ versus $\tan\beta$ for $m_0 = 1500$ GeV, $m_{1/2} = 160$ GeV, $A_0 = 0$ and $m_t = 175$ (as in de Boer *et al.*[13]), and $m_t = 171$ GeV (the central value of m_t as recently measured by D0 and CDF[28]). While $\Omega_{\tilde{Z}_1} h^2$ is too large for most of the range of $\tan\beta$, we see that it drops to the measured value around $\tan\beta = 52 - 55$. At this high a value of $\tan\beta$, the b and τ Yukawa couplings become very large, while the value of m_A drops (see Fig. 3). Even though $2m_{\tilde{Z}_1}$ is still far from the A resonance, annihilation through the virtual A^* becomes dominant enough to lower the relic density to WMAP-allowed values. The beauty of this approach is that when neutralino annihilation in the early universe via s -channel A exchange is large, so also is halo annihilation of neutralinos[29]. This contrasts with the case of $\tilde{Z}_1 \tilde{Z}_1 \rightarrow h \rightarrow b\bar{b}$, where early universe annihilation can be large, but $\langle\sigma v\rangle|_{v\rightarrow 0} \rightarrow 0$, so that the neutralino halo annihilation rate is small.

In Fig. 2b., we show the spin-independent neutralino-proton scattering cross section versus $\tan\beta$ for the same parameters as in Fig. 2a. We see that as $\tan\beta$ increases, the value of $\sigma_{SI}(\tilde{Z}_1 p)$ also increases. This is due to Higgs exchange direct detection scattering diagrams, and the increasing magnitude of the b -quark Yukawa coupling. The important point to notice,

LEP2 requires a SM-like h to have $m_h > 114.4$ GeV[27].

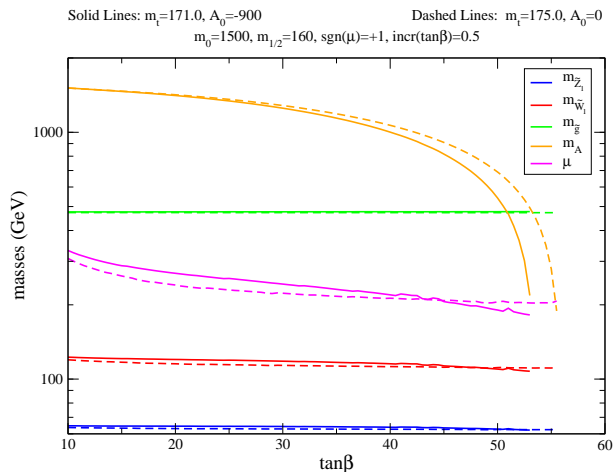


Figure 3: *Plot of sparticle masses versus $\tan\beta$ for the two cases of $mSUGRA$ model displayed in Table 1.*

however, is that the value of $\sigma_{SI}(\tilde{Z}_1 p)$ has increased into the Xenon-10 excluded region at a $\tan\beta$ value somewhat lower than that needed for the relic density to enter the WMAP-allowed dark matter band. Thus, technically, these cases for a SUSY interpretation of the Egret GeV anomaly would be excluded by the new Xenon-10 limits.

We list two WMAP-allowed $mSUGRA$ points in Table 1. The first, suggested in the de Boer *et al.* analysis[13] has $m_t = 175$ GeV so that an exact comparison can be made to Ref. [13]. The second point has m_t dialed down to 171 GeV in accord with recent top mass measurements at the Tevatron. In addition, for the second point, we take $A_0 = -900$ GeV which raises the value of m_h more closely into accord with LEP2 Higgs search limits. We see that both cases have $m_{\tilde{Z}_1} \sim 60$ GeV, while $m_{\tilde{g}} \sim 470$ GeV. Squarks and sleptons have masses above the TeV range. We also list in the Table the relic density $\Omega_{\tilde{Z}_1} h^2$, $BF(b \rightarrow s\gamma)$, the SUSY contribution to the muon anomalous magnetic moment Δa_μ , the branching fraction for $B_s \rightarrow \mu^+ \mu^-$ decay, $\sigma_{SI}(\tilde{Z}_1 p)$ in pb, and $\langle\sigma v\rangle|_{v \rightarrow 0}$. The neutralino-proton spin independent scattering cross section is $\sim 3 \times 10^{-7}$ pb in both cases— well above the Xenon-10 limit. The value of $\langle\sigma v\rangle|_{v \rightarrow 0} \sim 2 \times 10^{-26}$ cm³/sec, a value which gives sufficient halo annihilation in models assuming the de Boer DM halo profile.

We next wish to check if Xenon-10 would exclude *all* $mSUGRA$ interpretations of the Egret data. We do so by scanning over the entire $mSUGRA$ model parameter space:

$$\begin{aligned}
100 \text{ GeV} &< m_0 < 4000 \text{ GeV} \\
10 \text{ GeV} &< m_{1/2} < 1000 \text{ GeV} \\
-3000 \text{ GeV} &< A_0 < 3000 \text{ GeV} \\
1.1 &< \tan\beta < 60 \\
\mu &> 0.
\end{aligned} \tag{3}$$

Our results of this scan are plotted in Fig. 4. Here, we keep only points with $0.09 < \Omega_{\tilde{Z}_1} h^2 < 0.13$, and also $50 \text{ GeV} < m_{\tilde{Z}_1} < 70 \text{ GeV}$. Green points have a $BF(b \rightarrow s\gamma)$ in close accord

parameter	de Boer	mSUGRA(171)	NUHM
m_0	1500	1500	831.8
$m_{1/2}$	160	160	161.2
A_0	0	-900	-1597.1
$\tan \beta$	54.8	52.1	17.6
m_t	175	170.9	170.9
μ	203.5	177.5	644.0
$m_{\tilde{g}}$	472.3	476.9	450.8
$m_{\tilde{u}_L}$	1522.2	1522.8	891.1
$m_{\tilde{u}_R}$	1526.0	1526.5	914.4
$m_{\tilde{t}_1}$	897.1	890.7	248.3
$m_{\tilde{b}_1}$	1022.1	1025.0	632.2
$m_{\tilde{e}_L}$	1501.6	1501.6	853.6
$m_{\tilde{e}_R}$	1499.8	1499.8	802.4
$m_{\tilde{W}_1}$	110.9	106.3	131.7
$m_{\tilde{Z}_2}$	110.4	106.7	131.0
$m_{\tilde{Z}_1}$	62.4	61.8	66.6
m_A	309.1	347.0	157.0
m_h	113.6	112.8	116.6
$\Omega_{\tilde{Z}_1} h^2$	0.11	0.11	0.10
$BF(b \rightarrow s\gamma)$	3.0×10^{-4}	2.4×10^{-4}	3.1×10^{-4}
Δa_μ	10.3×10^{-10}	10.0×10^{-10}	5.4×10^{-10}
$BF(B_s \rightarrow \mu^+\mu^-)$	2.2×10^{-9}	9.3×10^{-9}	3.7×10^{-8}
$\sigma_{sc}(\tilde{Z}_1 p)$ [pb]	3.2×10^{-7}	3.1×10^{-7}	2.6×10^{-8}
$\langle \sigma v \rangle _{v \rightarrow 0}$ (cm^3/sec)	2.0×10^{-26}	2.3×10^{-26}	1.6×10^{-26}

Table 1: Masses and parameters in GeV units for three Egret-motivated benchmark points using Isajet 7.76.

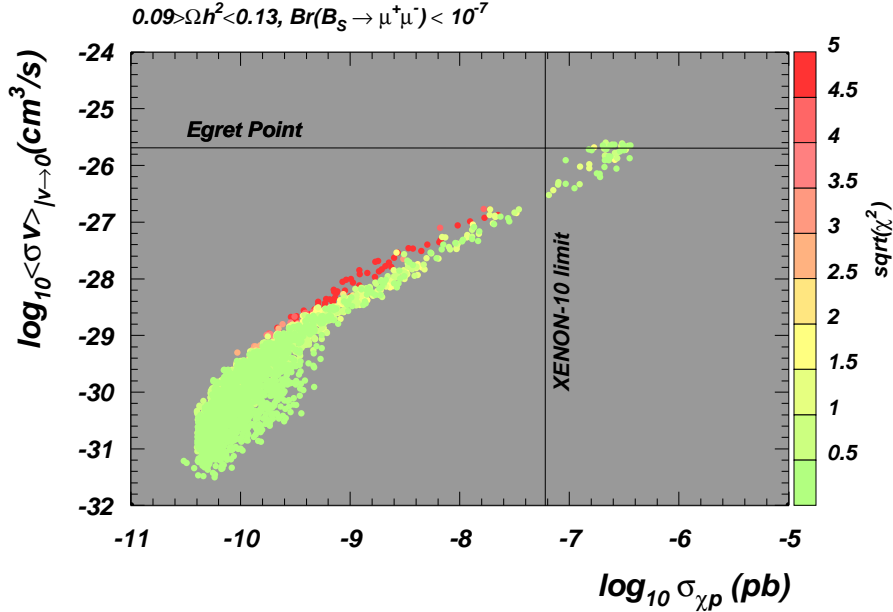


Figure 4: Scan of $mSUGRA$ parameter space for models which obey LEP2 constraints and have $0.09 < \Omega_{\tilde{Z}_1} h^2 < 0.13$. We plot results in the $\langle \sigma v \rangle|_{v \rightarrow 0}$ vs. $\sigma_{SI}(\tilde{Z}_1 p)$ plane. Green dots have good $BF(b \rightarrow s\gamma)$ while red dots deviate from the measured branching fraction.

with the measured value: $BF(b \rightarrow s\gamma) = (3.55 \pm 0.26) \times 10^{-4}$ from a combined analysis [30] of the CLEO, Belle and BABAR experiments. Yellow and especially red points give branching fractions further from the experimental central value. The surviving points are plotted in the $\langle \sigma v \rangle|_{v \rightarrow 0}$ vs. $\sigma_{SI}(\tilde{Z}_1 p)$ plane. We see that most points populate the low $\langle \sigma v \rangle|_{v \rightarrow 0}$ and low $\sigma_{SI}(\tilde{Z}_1 p)$ regions. These points come from either the stau co-annihilation region or the h -resonance annihilation region of the $mSUGRA$ model. There are no hyperbolic branch/focus point (HB/FP) contributions since $m_{\tilde{Z}_1} < M_W$, and so $\tilde{Z}_1 \tilde{Z}_1 \rightarrow W^+ W^-$ (as is enhanced in the HB/FP region) is kinematically forbidden. The points at large $\langle \sigma v \rangle|_{v \rightarrow 0} \sim 10^{-26}$ cm²/sec (so that they have a high halo annihilation rate into gammas) also are *all above the Xenon-10 dark matter limit!* For this reason, it seems an interpretation of the Egret GeV anomaly in terms of neutralino annihilation in the $mSUGRA$ model is ruled out. Of course, one way out is to assume we live in a local void of dark matter, and the local density is far below the assumed value of 0.3 GeV/cm³. One may also assume much lower local WIMP velocities, which would also lead to lower detection rates. (It may also be the case that we live in a locally overdense region, or that the velocity profile is harder than expected, leading to larger than expected DM detection rates.) Here, we will not further entertain these possibilities.

2.2 NUHM2 analysis

While the $mSUGRA$ model does not seem adequate to explain the Egret GeV anomaly in the face of the new Xenon-10 limit, other less restrictive supersymmetric models may do the job.

One highly motivated model beyond mSUGRA consists of models with non-universal soft SUSY breaking Higgs masses (NUHM). In simple $SO(10)$ SUSYGUT theories, the Higgs supermultiplets live in a $\mathbf{10}$ of $SO(10)$, while the matter supermultiplets live in the $\mathbf{16}$ dimensional spinor representation. Thus, one might naturally expect Higgs SSB terms to have different GUT scale masses than matter SSB terms (this is the one-parameter NUHM model, or NUHM1[31]). In $SU(5)$ SUSYGUT models, the doublet \hat{H}_u lives in a $\mathbf{5}$, while the doublet \hat{H}_d lives in a $\bar{\mathbf{5}}$. In this case, both $m_{H_u}^2$ and $m_{H_d}^2$ can be taken as independent parameters, whereas the matter scalars remain unified to m_0 . This is the two-parameter NUHM model, or NUHM2[32]. In NUHM2, the GUT scale parameters $m_{H_u}^2$ and $m_{H_d}^2$ can be traded for independent weak scale parameters μ and m_A (whereas in mSUGRA, these quantities are derived from the GUT scale inputs, mainly m_0). Here, we will examine the NUHM2 model, with parameter space given by

$$m_0, m_{1/2}, A_0, \mu, m_A, \tan \beta, \quad (4)$$

where we take $m_t = 171$ GeV as usual. Our goal will be to lower $\tan \beta$, so that we will diminish the direct detection cross section to levels below the Xenon-10 limit. Meanwhile, we wish to maintain a large $\langle \sigma v \rangle|_{v \rightarrow 0}$ so that we maintain a high rate of neutralino halo annihilations. This can be done by lowering m_A so that we move nearer (but not directly on) A -resonance annihilation.

Here, we scan over the NUHM2 parameter space:

$$\begin{aligned} 100 \text{ GeV} &< m_0 < 2000 \text{ GeV} \\ 50 \text{ GeV} &< m_{1/2} < 300 \text{ GeV} \\ -3000 \text{ GeV} &< A_0 < 3000 \text{ GeV} \\ 1.1 &< \tan \beta < 60 \\ 50 \text{ GeV} &< \mu < 1000 \text{ GeV} \\ 70 \text{ GeV} &< m_A < 500 \text{ GeV}, \end{aligned} \quad (5)$$

while again plotting points which satisfy the WMAP relic density bound and have $50 \text{ GeV} < m_{\tilde{Z}_1} < 70 \text{ GeV}$. The points are again plotted in the $\langle \sigma v \rangle|_{v \rightarrow 0}$ vs. $\sigma_{SI}(\tilde{Z}_1 p)$ plane in Fig. 5. In this case, we *do* find a collection of points with simultaneously the correct relic abundance and neutralino mass, a high rate of halo annihilation (since $\langle \sigma v \rangle|_{v \rightarrow 0} \sim 10^{-26} \text{cm}^3/\text{sec}$), and with $\sigma_{SI}(\tilde{Z}_1 p)$ below the Xenon-10 limit! While the collection of points does satisfy the Xenon-10 limit, note that they do not extend to arbitrarily small values of $\sigma_{SI}(\tilde{Z}_1 p)$. In fact, one prediction is that if the NUHM2 SUGRA model is to explain the Egret GeV anomaly, then $\sigma_{SI}(\tilde{Z}_1 p) \gtrsim 10^{-8}$ pb, which is well within range of a number of upcoming direct detection experiments, including Lux, Xenon-100, WARP-140 and mini-CLEAN.

As an example of a NUHM2 point which satisfies all constraints, we list the third point in Table 1: a point with $m_0 = 831.8$ GeV and $m_{1/2} = 161.2$ GeV. Like the mSUGRA models, it has a light gluino, with $m_{\tilde{g}} \sim 450$ GeV. It also has $m_A \sim 157$ GeV, which is generically below the mSUGRA models, which predict $m_A \sim 200 - 400$ GeV. The $\tan \beta$ value is just 17.6, so the b -Yukawa coupling is not so large, and the A -width is rather narrow.

To show explicitly the range of $m_{\tilde{g}}$ and m_A expected in our scans, we plot in Fig. 6 points from a). the mSUGRA scan and b). the NUHM2 scan in the m_A vs. $m_{\tilde{g}}$ plane. In both cases,

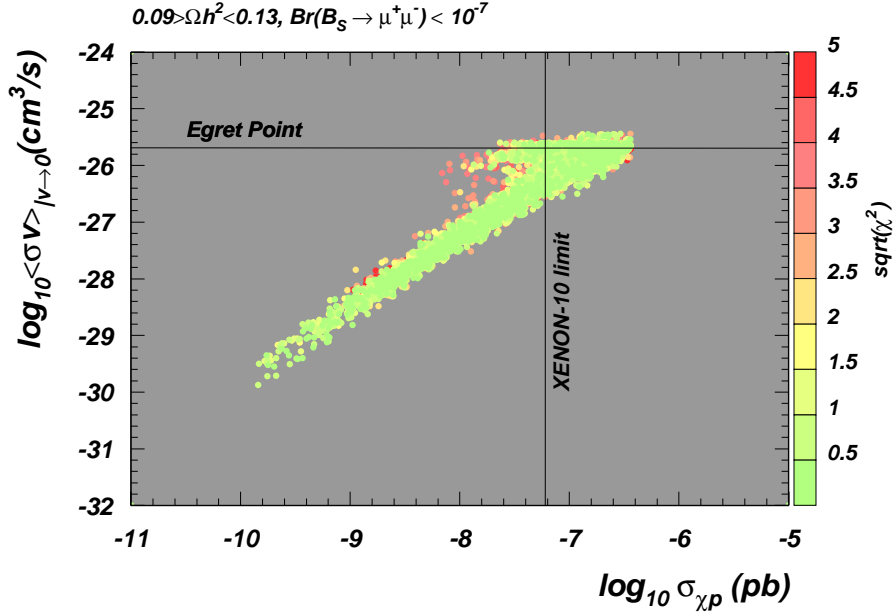


Figure 5: Scan of NUHM2 parameter space for models which obey LEP2 constraints and have $0.09 < \Omega_{\tilde{Z}_1} h^2 < 0.13$. We plot results in the $\langle \sigma v \rangle|_{v \rightarrow 0}$ vs. $\sigma_{SI}(\tilde{Z}_1 p)$ plane. Green dots have good $BF(b \rightarrow s\gamma)$ while red dots deviate from the measured branching fraction.

surviving points have $m_{\tilde{Z}_1} : 50 - 70$ GeV and $0.09 < \Omega_{\tilde{Z}_1} h^2 < 0.13$, $BF(B_s \rightarrow \mu^+ \mu^-) < 10^{-7}$ and further, we require $\langle \sigma v \rangle|_{v \rightarrow 0} > 10^{-26}$ cm³/sec so that there is sufficient halo annihilation to explain the Egret excess. The points in the mSUGRA case all have $m_{\tilde{g}} \sim 400 - 550$ GeV, while $m_A > 200$ GeV. In the NUHM2 case, we further require $\sigma_{SI}(\tilde{Z}_1 p) < 6 \times 10^{-8}$ pb. Here, we see a similar range of $m_{\tilde{g}}$ is allowed. However, in the NUHM2 case, we always have $m_A < 200$ GeV. This is an important distinction between the two interpretations which can be directly tested/measured at LHC.

3 Egret SUSY interpretation and the LHC

The CERN LHC is expected to turn on in mid-2008, and gradually begin accumulating data into 2009. It is not unreasonable to expect of order 0.1 fb^{-1} of integrated luminosity in the first full year of running.

If the SUSY interpretation of the Egret GeV anomaly is correct, then we expect the DM particle to be a neutralino of mass $m_{\tilde{Z}_1} \simeq 50 - 70$ GeV. Most SUSY models also assume gaugino mass unification at the GUT scale. In such models, the gluino mass is expected to be $m_{\tilde{g}} \sim 7M_1$, and if the \tilde{Z}_1 is dominantly bino-like, with $\mu \gg M_1$, then we expect $m_{\tilde{Z}_1} \sim M_1$ and thus would predict $m_{\tilde{g}} \sim 350 - 500$ GeV. Squarks and sleptons can be considerably heavier, as is the case in the points listed in Table 1. In this type of scenario, we would expect new physics events from SUSY at the CERN LHC to be dominated by gluino pair production, followed by gluino cascade decays[33]. The cross section for $pp \rightarrow \tilde{g}\tilde{g}X$ at the LHC for the above range of

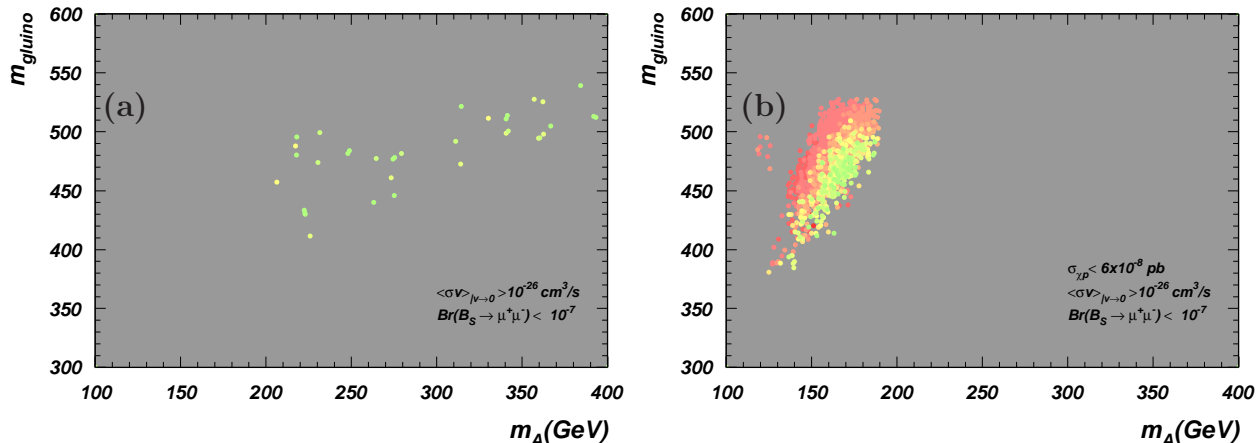


Figure 6: Scan of a). *mSUGRA* model and b). *NUHM2* model parameter space for points which obey LEP2 constraints and have $0.09 < \Omega_{\tilde{Z}_1} h^2 < 0.13$ and $\langle\sigma v\rangle_{|v\rightarrow 0} > 10^{-26} \text{ cm}^3/\text{sec}$. We plot results in the $m_{\tilde{g}}$ vs. m_A plane. Green dots have good $BF(b \rightarrow s\gamma)$ while red dots deviate from the measured branching fraction.

gluino masses is $\sim 10^4 - 10^5 \text{ fb}$ [34]. Thus, with just 0.1 fb^{-1} of integrated luminosity, we can already expect $10^3 - 10^4$ gluino pair events to be recorded per LHC experiment.

While new physics may be lurking in the LHC already shortly after turn-on, it is unclear whether the detectors will be fully calibrated to allow for a new physics search. For instance, traditional SUSY searches rely on a $E_T^{\text{miss}} + jets$ signature, where large E_T^{miss} is required to reject SM background events from the SUSY signal. To properly use the E_T^{miss} variable, a full knowledge of the detector is required, since E_T^{miss} can not only arise from signal and background events, but also from 1. dead regions of the detector, 2. “hot”, or mis-firing calorimeter cells, 3. cosmic ray events and 4. energy mis-measurement in active calorimeter cells. In Ref. [35], it was recently pointed out that early discovery of SUSY at the LHC was possible *without* using E_T^{miss} , and that a reach in $m_{\tilde{g}}$ to $600 - 700 \text{ GeV}$ could be attained without using E_T^{miss} , and with only 0.1 fb^{-1} of integrated luminosity. Effectively, the idea was to make use of multi-lepton production[36] in the lengthy sparticle cascade decays. Thus, requiring ≥ 4 jets production along with ≥ 2 or 3 isolated leptons, allowed for an excellent rejection of SM background (dominated by $t\bar{t}$ production) compared to signal so that a SUSY discovery could be made. The values of $m_{\tilde{g}}$ expected from the SUSY interpretation of the Egret GeV anomaly fall well within this “early discovery” range.

Here, we use the same detector simulation, jet finding algorithm and lepton isolation criterion as detailed in Ref. [35], and adopt the same set of SM background events from QCD jet production, $W + jets$, $Z + jets$, $t\bar{t}$ production and vector boson pair production. We require first that signal and background events satisfy the set of cuts $C1'$: *i*). $n(jets) \geq 4$, *ii*). $E_T(j1, j2, j3, j4) > 100, 50, 50, 50 \text{ GeV}$, respectively (where jets are ordered according to E_T value) and *iii*). transverse sphericity $S_T \geq 0.2$. We then plot a multiplicity of isolated leptons (a lepton $\ell = e$ or μ is isolated if it has $E_T(\ell) > 20 \text{ GeV}$, $|\eta(\ell)| < 2.5$ and $\sum E_T^{\text{cells}} < 5 \text{ GeV}$ in

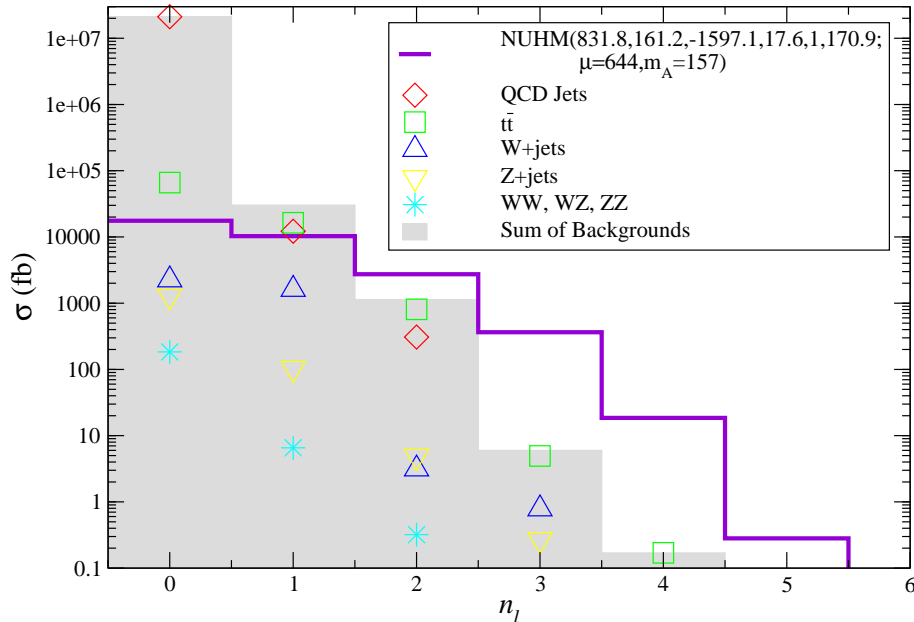


Figure 7: *Distribution in number of isolated leptons from the NUHM2 point in Table 1 after cuts C1'. We also show component SM backgrounds and the summer SM background (gray histogram).*

a cone of $\Delta R \equiv \sqrt{\Delta\eta^2 + \Delta\phi^2} < 0.2$ about the lepton direction). The results are shown in Fig. 7. Here, we see that SM background dominates signal for $n_\ell = 0$ or 1. But already at $n_\ell = 2$, the signal from the NUHM2 point in Table 1 stands out above background. At $n_\ell = 3$, there still remains ~ 400 fb of signal, while BG is negligible. Given these results, it seems that the SUSY interpretation of the Egret GeV anomaly should be easily testable at the LHC after only 0.1 fb^{-1} of integrated luminosity is obtained, and even before the detectors are fully calibrated such that they can perform a reliable search for $E_T^{\text{miss}} + jets$ events.

Once a SUSY signal is obtained, then the set of likely signal events can be scrutinized to try to reconstruct sparticle masses, etc. The starting point is often to first look at the opposite sign/same flavor (OS/SF) dilepton invariant mass spectrum $m(\ell\bar{\ell})$ [37]. We plot the distribution $d\sigma/dm(\ell\bar{\ell})$ in Fig. 8 arising from the second mSUGRA point in Table 1, after cuts C1' and requiring a pair of OS/SF isolated leptons. In this case, a clear mass edge is seen at $m_{\tilde{Z}_2} - m_{\tilde{Z}_1} = 44.9$ GeV. There is also a Z peak in both signal and BG (the latter arising because Isajet includes W and Z radiation in its parton shower algorithm).

In the case of the NUHM2 model from Table 1, the \tilde{t}_1 mass is so light that $\tilde{g} \rightarrow t\tilde{t}_1$ dominantly, and the \tilde{Z}_2 production via cascade decays is somewhat suppressed. Furthermore, the $\tilde{Z}_2 \rightarrow \tilde{Z}_1 e^+ e^-$ branching fraction is suppressed to the 0.8% level; in this case, the suppression is due to the presence of relatively light A and H Higgs bosons, which enhance the decay $\tilde{Z}_2 \rightarrow \tilde{Z}_1 b\bar{b}$ to the 45% level, at the expense of first/second generation decay modes. Thus, in the $m(\ell\bar{\ell})$ distribution for NUHM2 shown in Fig. 9, we see a continuum distribution instead of a distinct mass edge (the mass edge would occur at $m_{\tilde{Z}_2} - m_{\tilde{Z}_1} = 64.4$ GeV in this case). The

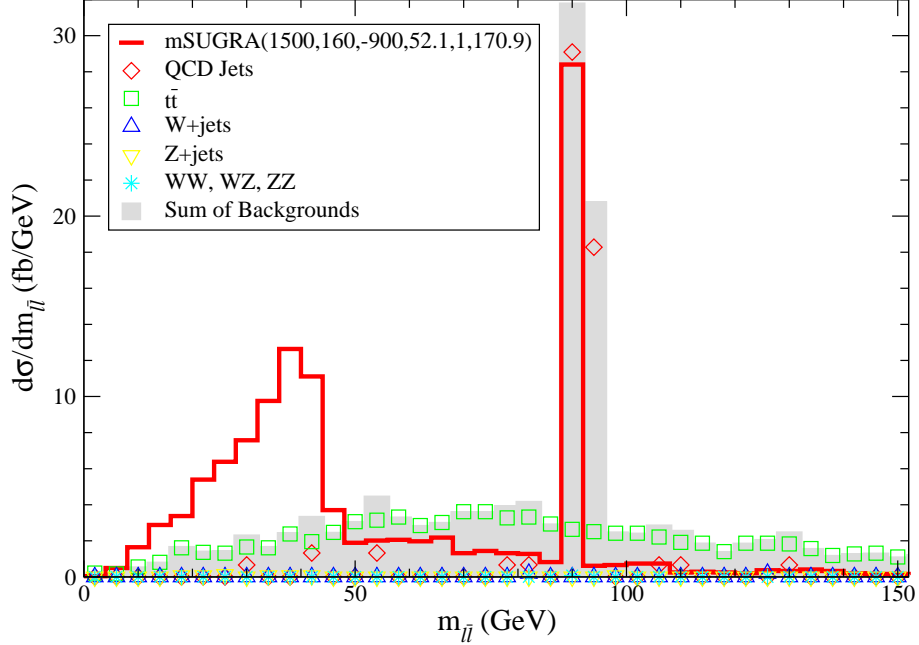


Figure 8: *Distribution in OS/SF dilepton invariant mass from the second mSUGRA point in Table 1 after cuts C1'. We also show component SM backgrounds and the sum of SM background (gray histogram).*

other crucial observable to test between a mSUGRA or NUHM2 interpretation of the Egret excess will come from the LHC measurement of the heavy Higgs boson mass spectrum. The ATLAS and CMS groups have posted reach plots for MSSM Higgs bosons in the m_A vs. $\tan\beta$ plane [38, 39]. The H and A Higgs bosons should be seeable in the $b\bar{b}$, $\tau\bar{\tau}$ and even $\mu^+\mu^-$ modes [40] in the NUHM2 model for $\tan\beta \gtrsim 6$ since $m_A \lesssim 200$ GeV, and their masses should be measurable. The mSUGRA interpretation requires $\tan\beta \sim 50$ and has relatively light m_A as well, and should likewise be visible, but with mass $m_A \gtrsim 200$ GeV. In Fig. 10, we present the mSUGRA a). and NUHM2 b). points in the $(\tan\beta, m_A)$ plane with lightest neutralino mass in the range of 50-70 GeV. Points obey LEP2 constraints and have $0.09 < \Omega_{\tilde{Z}_1} h^2 < 0.13$, $\langle\sigma v\rangle|_{v\rightarrow 0} > 10^{-26}$ cm³/sec and $Br(B_S \rightarrow \mu^+\mu^-) < 10^{-7}$. For NUHM2 parameter space we also require $\sigma_{SI}(\tilde{Z}_1 p) < 6^{-8}$ pb to satisfy the Xenon-10 limit. One can clearly see that indeed these scenarios suggest a very distinctive A -Higgs boson phenomenology. Recent Tevatron limits [41] for the $(\tan\beta, m_A)$ plane already exclude $m_A < 180$ for $\tan\beta \geq 50$. So, the Tevatron can test now a small part of NUHM2 parameter space with large values of $\tan\beta$, while parameter space with $100 < m_A < 200$ and $\tan\beta \leq 30$ could be tested and completely covered only at the LHC.

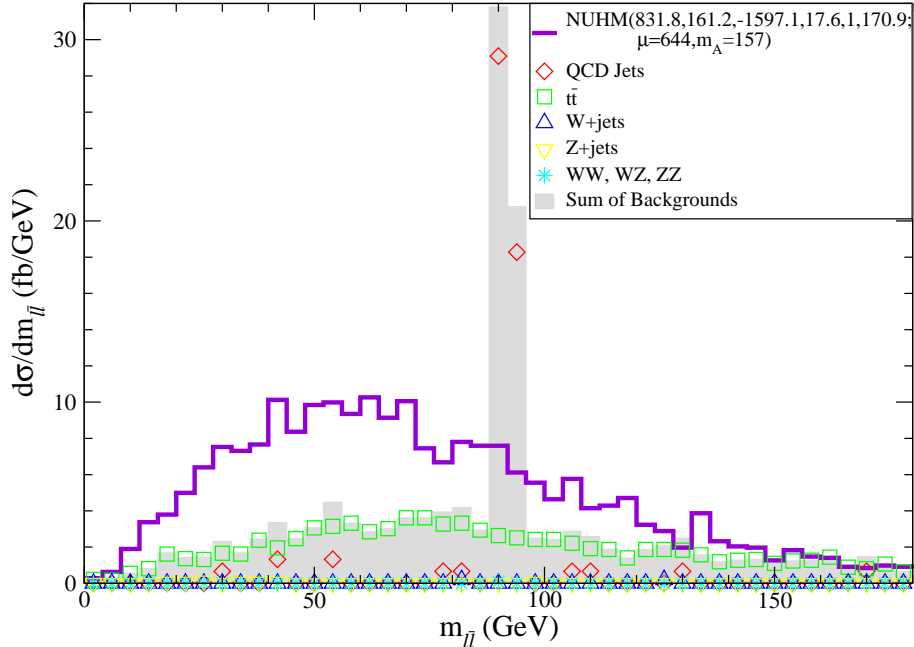


Figure 9: *Distribution in OS/SF dilepton invariant mass from the NUHM2 point in Table 1 after cuts C1'. We also show component SM backgrounds and the sum of SM background (gray histogram).*

4 Conclusions

In this paper, we have examined the SUSY interpretation of the Egret GeV anomaly. The SUSY interpretation requires $m_{\tilde{Z}_1} \sim 50 - 70$ GeV, and a relic density of $\Omega_{\tilde{Z}_1} h^2 \sim 0.1$. In order to satisfy these criteria, while maintaining a large halo annihilation rate for $\tilde{Z}_1 \tilde{Z}_1 \rightarrow A^* \rightarrow b\bar{b}$, one must move to very large $\tan\beta \sim 52 - 55$ in the context of the mSUGRA model. At this high $\tan\beta$, the predicted spin-independent $\tilde{Z}_1 p$ scattering cross section exceeds recent limits from the Xenon-10 collaboration.

In order to maintain a SUSY interpretation of the Egret GeV anomaly, we suggest moving to SUSY models with a non-universal Higgs sector: the NUHM2 model. In this case, with freedom to adjust the value of m_A , one can reduce the value of $\tan\beta$ so that the predicted $\sigma_{SI}(\tilde{Z}_1 p)$ is lowered below Xenon-10 limits, but maintain a valid relic density and halo annihilation rate by lowering m_A to values below 200 GeV. If the SUSY interpretation of the Egret GeV anomaly is correct, then we predict direct detection cross sections $\sigma_{SI}(\tilde{Z}_1 p) \gtrsim 10^{-8}$ pb, which should be accessible to the next round of DD experiments. Further, the gluino mass should be in the range 400 – 550 GeV, and should be seeable in the multi-jet plus multi-lepton channel at LHC with just 0.1 fb^{-1} of integrated luminosity. A dilepton mass edge in these signal events may not be apparent since the light Higgs spectrum enhances \tilde{Z}_2 decay to third generation fermions at the expense of first/second generation leptons. Since $m_{A,H} \lesssim 200$ GeV, the A and H should be readily visible at LHC via searches for $A, H \rightarrow b\bar{b}, \tau^+\tau^-$ or $\mu^+\mu^-$, even for relatively low

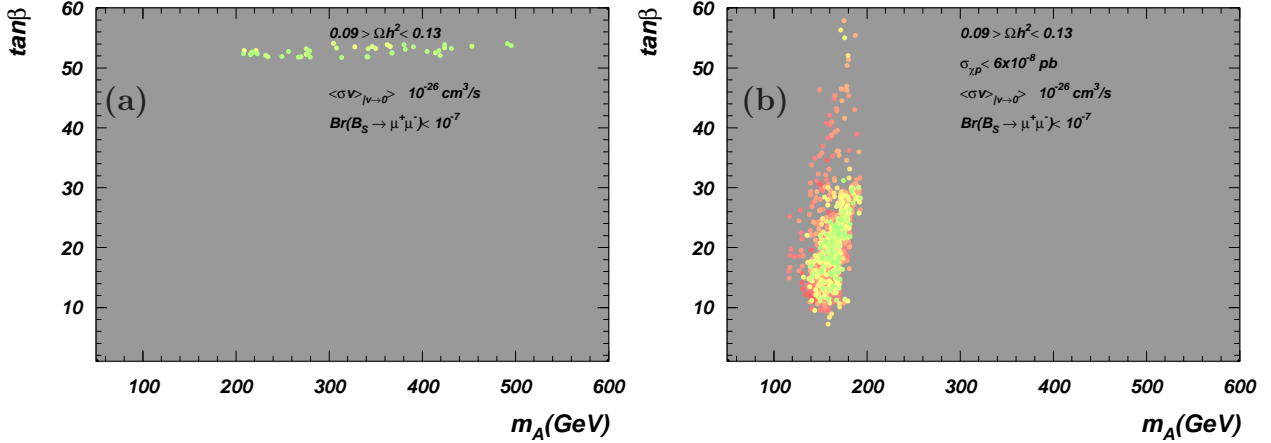


Figure 10: Points from a). $mSUGRA$ and b). $NUMH2$ interpretation of the Egret GeV anomaly in $(\tan\beta, m_A)$ plane with lightest neutralino mass in the range of 50-70 GeV. Points obey LEP2 constraints and have $0.09 < \Omega_{\tilde{Z}_1} h^2 < 0.13$, $\langle \sigma v \rangle|_{v \rightarrow 0} > 10^{-26} \text{ cm}^3/\text{sec}$ and $Br(B_S \rightarrow \mu^+ \mu^-) < 10^{-7}$. For $NUMH2$ parameter space we also require $\sigma_{SI}(\tilde{Z}_1 p) < 6 \times 10^{-8} \text{ pb}$ to satisfy Xenon-10 limit. Green dots have good $BF(b \rightarrow s\gamma)$ while red dots deviate from the measured branching fraction.

values of $\tan\beta \gtrsim 6 - 10$. This observation clearly distinguishes between the $mSUGRA$ and $NUMH2$ interpretations of the Egret GeV anomaly.

Acknowledgments

We gratefully acknowledge Professor W. de Boer for various discussions.

References

- [1] See *e.g.* C. Jungman, M. Kamionkowski and K. Griest, *Phys. Rept.* **267** (195) 1996; more recent reviews can be found in A. Lahanas, N. Mavromatos and D. Nanopoulos, *Int. J. Mod. Phys. D* **12** (2003) 1529; M. Drees, hep-ph/0410113; K. Olive, ‘‘Tasi Lectures on Astroparticle Physics’’, astro-ph/0503065.
- [2] D. N. Spergel *et al.* (WMAP Collaboration), astro-ph/0603449 (2006).
- [3] S. Heinemeyer, arXiv:0710.3022 [hep-ph].
- [4] H. Baer, A. Belyaev, T. Krupovnickas and J. O’Farrill, *JCAP***0408** (2004) 005.
- [5] D. S. Akerib *et al.* (CDMS Collaboration), astro-ph/0405033 (2004).
- [6] J. Angle *et al.* (XENON collaboration) arXiv:0706.0039 (2007) [astro-ph].
- [7] H. Baer and X. Tata, *Weak Scale Supersymmetry: From Superfields to Scattering Events*, (Cambridge University Press, 2006).

- [8] For a review, see D. Hooper and S. Profumo, *Phys. Rep.* **453** (2007) 29.
- [9] For a review, see M. Perelstein, *Pramana* **67**, 813 (2006) [arXiv:hep-ph/0703138].
- [10] P. Sreekumar *et al.* [EGRET Collaboration], *Astrophys. J.* **494**, 523 (1998) [arXiv:astro-ph/9709257].
- [11] W. de Boer, M. Herold, C. Sander, V. Zhukov, A. V. Gladyshev and D. I. Kazakov, arXiv:astro-ph/0408272.
- [12] W. de Boer, C. Sander, V. Zhukov, A. V. Gladyshev and D. I. Kazakov, *Astron. Astrophys.* **444**, 51 (2005) [arXiv:astro-ph/0508617].
- [13] W. de Boer, C. Sander, V. Zhukov, A. Gladyshev and D. Kazakov, *Phys. Lett. B* **636** (2006) 13.
- [14] S. Dimopoulos and H. Georgi, *Nucl. Phys. B* **193** (1981) 150; A. Chamseddine, R. Arnowitt and P. Nath, *Phys. Rev. Lett.* **49** (1982) 970; R. Barbieri, S. Ferrara and C. Savoy, *Phys. Lett. B* **119** (1982) 343; N. Ohta, *Prog. Theor. Phys.* **70** (1983) 542; L. J. Hall, J. Lykken and S. Weinberg, *Phys. Rev. D* **27** (1983) 2359; for reviews, see H. P. Nilles, *Phys. Rep.* **110** (1984) 1, and P. Nath, hep-ph/0307123.
- [15] Talk by W. de Boer, in the *Proceedings of the 2005 International Linear Collider Physics and Detector Workshop and 2nd ILC Accelerator Workshop*, Snowmass, Colorado, 14-27 Aug 2005, Published in ECONF C0508141:ALCPG0502,2005.
- [16] M. Drees and M. Nojiri, *Phys. Rev. D* **47** (1993) 376; H. Baer and M. Brhlik, *Phys. Rev. D* **53** (1996) 597 and *Phys. Rev. D* **57** (1998) 567; H. Baer, M. Brhlik, M. Diaz, J. Ferrandis, P. Mercadante, P. Quintana and X. Tata, *Phys. Rev. D* **63** (2001) 015007; J. Ellis, T. Falk, G. Ganis, K. Olive and M. Srednicki, *Phys. Lett. B* **510** (2001) 236; L. Roszkowski, R. Ruiz de Austri and T. Nihei, *J. High Energy Phys.* **0108** (024) 2001; A. Djouadi, M. Drees and J. L. Kneur, *J. High Energy Phys.* **0108** (2001) 055; A. Lahanas and V. Spanos, *Eur. Phys. J. C* **23** (2002) 185; H. Baer and C. Balazs, *JCAP***0305** (2003) 006; see also Ref. [24].
- [17] For a summary, see *e.g.* D. Hooper, arXiv:0710.2062 [hep-ph].
- [18] A. Strong, I. Moskalenko and O. Reimer, *Astrophys. J.* **613** (2004) 962.
- [19] F. W. Stecker, S. D. Hunter and D. A. Kniffen, arXiv:0705.4311 [astro-ph].
- [20] L. Bergstrom, J. Edsjo, M. Gustafsson and P. Salati, *JCAP***0605** (2006) 006.
- [21] W. de Boer, I. Gebauer, C. Sander, M. Weber and V. Zhukov, *AIP Conf. Proc.* **903**, 607 (2007) [arXiv:astro-ph/0612462].
- [22] ISAJET v7.74, by H. Baer, F. Paige, S. Protopopescu and X. Tata, hep-ph/0312045.
- [23] H. Baer, J. Ferrandis, S. Kraml and W. Porod, *Phys. Rev. D* **73** (2006) 015010.
- [24] H. Baer, C. Balazs and A. Belyaev, *J. High Energy Phys.* **0203** (2002) 042; H. Baer, C. Balazs, A. Belyaev, J. K. Mizukoshi, X. Tata and Y. Wang, *J. High Energy Phys.* **0207** (2002) 050.
- [25] See <http://dmtools.berkeley.edu/limitplots/> by R. Gaitskell and J. Filippini.

- [26] H. Baer, C. Balazs, A. Belyaev and J. O’Farrill, *JCAP* **0309**, 007 (2003) [arXiv:hep-ph/0305191].
- [27] S. Schael *et al.* [ALEPH, DELPHI, L3 and OPAL Collaborations and LEP Working Group for Higgs Boson Searches], *Eur. Phys. J. C* **47** (2006) 547 [hep-ex/0602042].
- [28] CDF and D0 collaborations, hep-ph/0703034 (2007)
- [29] H. Baer and J. O’Farrill, *JCAP* **0404**, 005 (2004) [arXiv:hep-ph/0312350].
- [30] E. Barberio *et al.* (Heavy Flavor Averaging Group), hep-ex/0603003.
- [31] H. Baer, A. Mustafayev, S. Profumo, A. Belyaev and X. Tata, *Phys. Rev. D* **71** (2005) 095008.
- [32] V. Berezinsky *et al.*, *Astropart. Phys.* **5** (1996) 1; P. Nath and R. Arnowitt, *Phys. Rev. D* **56** (1997) 2820; A. Bottino *et al.* *Phys. Rev. D* **59** (1999) 095004 and *Phys. Rev. D* **63** (2001) 125003; J. Ellis, K. Olive and Y. Santoso, *Phys. Lett. B* **539** (2002) 107; J. Ellis, T. Falk, K. Olive and Y. Santoso, *Nucl. Phys. B* **652** (2003) 259; H. Baer, A. Mustafayev, S. Profumo, A. Belyaev and X. Tata, *J. High Energy Phys.* **0507** (2005) 065; C. Lester, A. Parker and M. J. White, hep-ph/0609298; L. Solmaz, hep-ph/0609162.
- [33] H. Baer, J. Ellis, G. Gelmini, D. Nanopoulos and X. Tata, *Phys. Lett. B* **161** (1985) 175; G. Gamberini, *Z. Physik C* **30** (1986) 605; H. Baer, V. Barger, D. Karatas and X. Tata, *Phys. Rev. D* **36** (1987) 96; R. M. Barnett, J. F. Gunion and H. Haber, *Phys. Rev. D* **37** (1988) 1892; H. Baer, X. Tata and J. Woodside, *Phys. Rev. D* **42** (1990) 1568; A. Bartl, W. Majerotto, B. Mösslacher, N. Oshimo and S. Stippel, *Phys. Rev. D* **43** (1991) 2214; H. Baer, M. Bisset, X. Tata and J. Woodside, *Phys. Rev. D* **46** (1992) 303. A. Bartl, W. Majerotto and W. Porod, *Z. Physik C* **64** (1994) 499; A. Djouadi, Y. Mambrini and M. Mühlleitner, *Eur. Phys. J. C* **20** (2001) 563; J. Hisano, K. Kawagoe and M. Nojiri, *Phys. Rev. D* **68** (2003) 035007.
- [34] See *e.g.* H. Baer, C. H. Chen, F. Paige and X. Tata, *Phys. Rev. D* **52** (1995) 2746; H. Baer, T. Krupovnickas, S. Profumo and P. Ullio, *J. High Energy Phys.* **0510** (2005) 020.
- [35] H. Baer, H. Prosper and H. Summy, arXiv:0801.3799 [hep-ph].
- [36] H. Baer, X. Tata and J. Woodside, *Phys. Rev. D* **45** (1992) 142.
- [37] H. Baer, K. Hagiwara and X. Tata, *Phys. Rev. D* **35** (1987) 1598; H. Baer, D. Dzialo-Karatas and X. Tata, *Phys. Rev. D* **42** (1990) 2259; H. Baer, C. Kao and X. Tata, *Phys. Rev. D* **48** (1993) 5175; H. Baer, C. H. Chen, F. Paige and X. Tata, *Phys. Rev. D* **50** (1994) 4508; I. Hinchliffe *et al.*, *Phys. Rev. D* **55** (1997) 5520 and *Phys. Rev. D* **60** (1999) 095002; H. Bachacou, I. Hinchliffe and F. Paige, *Phys. Rev. D* **62** (2000) 015009; Atlas Collaboration, LHCC 99-14/15; C. Lester, M. Parker and M. White, *J. High Energy Phys.* **0601** (2006) 080.
- [38] See *e.g.* C. Collins-Tooth [ATLAS Collaboration], arXiv:0712.1509 [hep-ex].
- [39] R. Kinnunen [CMS Collaboration], *Acta Phys. Slov.* **55** (2005) 037.
- [40] S. Dawson, D. Dicus and C. Kao, *Phys. Lett. B* **545** (2002) 132 and S. Dawson, D. Dicus, C. Kao and R. Malhotra, *Phys. Rev. Lett.* **92** (2004) 241801.
- [41] Talk of A. Anastassov at Aspen 2008 Winter Conference, 13-19 January 2008, Aspen, Colorado <http://www-cdf.fnal.gov/physics/alltran.html>